ISSN 2350-1022

International Journal of Recent Research in Mathematics Computer Science and Information Technology
Vol. 7, Issue 1, pp: (32-43), Month: April 2020 – September 2020, Available at: www.paperpublications.org

Mathematical Modeling of Shiga Toxin Incorporating the Environment

Serapia Peter Soka[1], Dr. Mary Wainaina[2], Dr. Isaac Mwangi[3]

[1, 2, 3] Department of Mathematica and Actuarial Science, Catholic University of Eastern Africa, Nairobi Kenya

Abstract: **Escherichia coli is species of bacteria which can be grouped into two types: One that causes illness to human beings and second group is a harmless bacterium. The harmful ones cause disease by producing toxin known as Shiga toxin; they are called Shiga toxin producing Escherichia coli. In this project, a model consisting of three sub populations which named; susceptible population S(t), Infected population I(t) and recovered population R(t). Differential equations were formulated from the model. Disease free equilibrium and Endemic equilibrium were determined from the model equations. The disease-free equilibrium was determined to be asymptotically stable when $R_0 < 1$ and unstable otherwise. The basic reproductive number (R_0) was computed using Next generation method. Through sensitivity analysis, the most sensitive parameter to the basic reproductive number was determined. Numerical simulation of the model equations was done.**

Keywords: **Shiga Toxin, Model, Reproductive Number, Numerical Simulation, Equilibrium, Sensitivity, Analysis.**

1. INTRODUCTION

Escherichia coli (E. coli) is a species of bacteria which could be divided into two types: one that causes illness to human beings, and one that is harmless. This species is among the leading causes of common infections from bacteria. Such infections include travellers' diarrhoea, urinary tract infection (UTI), Haemolytic Uremic Syndrome (HUS), Cholecystitis and Cholangitis [1]. The harmful bacteria cause diseases by producing toxin known as Shiga toxin. They know as *Shiga Toxin producing Escherichia coli* (STEC) *Verocytotoxin E.coli* (VTEC)or *Enterohemorrhagic E.coli* (EHEC).

Haemolytic Uremic Syndrome (HUS) is a life-threatening disease which is caused by Shiga toxin producing bacteria. Cattle are considered to be natural reservoir of the pathogens and they act as a major source of human infection. This takes place directly or indirectly through their products. STEC 015:H7 is recognized to be the pathogen with the greatest impact on public health, with various serotype (STEC) identified worldwide [2].

Majority of outbreaks of STEC arise from the consumption of contaminated food such as milk, fruits, meat, raw vegetables and water [4]. Most of the food borne pathogens live in the gastrointestinal tract of animals, so the main route of pathogen excretion is through faecal shedding [5]. Due to indirect contact with farm and petting zoo environment or direct contact with animals' outbreaks can occur. The main reservoirs of *Shiga Toxin producing Escherichia coli* are mostly raw milk, under cooked beef, the intestinal tracts of healthy cattle and food products from these sources that are poorly handled [11]. Cattle that are colonized by shedding Escherichia coli are not only the source of food contamination at slaughter, but their manure may also contaminate fruits and vegetables when used as fertilizer [7]. Spreading of *Shiga Toxin producing Escherichia coli* to human beings occur merely when they consume contaminated food. In Scotland, a large population in rural areas have been at great risk of vulnerability to *Shiga Toxin producing Escherichia coli* due to their great exposure to animals and their waste product like faeces and urine [9]. *Shiga Toxin producing Escherichia coli* has been discovered in most developed countries to be the source of disease outbreaks. These outbreaks are of great concern in health care programs. Two-thirds of the outbreaks related with food-borne illness caused by *Shiga Toxin producing Escherichia coli* in United State of America were due to consumption of raw vegetables [12].

The largest catastrophe was caused by *Shiga Toxin producing Escherichia coli* faced Germany in 2011, whereby 3842 cases were reported. The laboratory results confirmed Escherichia coli gastroenteritis (fever, vomiting, lack of appetite, diarrhoea) among 2987 cases. Among 855 people who reported having Haemolytic Uremic Syndrome (HUS); 35 of them died [13].

ISSN 2350-1022

International Journal of Recent Research in Mathematics Computer Science and Information Technology
Vol. 7, Issue 1, pp: (32-43), Month: April 2020 – September 2020, Available at: www.paperpublications.org

In Tanzania, cattle and goats are accommodated together in residential areas. The animal excreta produced overnight is removed by hoes or bare hands and accumulated near the residential areas. During the day, graze together in the same area. During grazing, the infected cattle transmit the bacteria to the environment through their excreta. During hot seasons, there are large outbreaks caused by *Shiga Toxin producing Escherichia coli* due to the sharing of common sources of drinking water between human beings and livestock. The serotype that is found in Tanzania specifically in cattle and water are mostly E. coli 0157:H7 and *Enteropathogenic E. coli* (EPEC) [14].

Diarrheal and urinary tract infection (UTI) are consequences of outbreaks caused by *Shiga Toxin producing Escherichia coli* in under developed countries. 64.5% and 70% of UTI which were reported in Kenya and North-Western Tanzania respectively were caused by Escherichia coli infections. Likewise, in North- Eastern Tanzania, children under 5 years old and aged people were discovered to be victims of UTI [14].

A cross-section study of urban and preurban livestock was carried out in Morogoro. It was done by isolating and characterizing Non-Sorbitol fermenting (NSF) Escherichia coli. The samples collected were water, soil, human stool and faeces from cattle. Questionnaires were used for interviews and the questions were meant to find out the management practices concerning cattle and manure. The sorbitol MacConkey agar was used to isolate and characterize Escherichia coli by conventional biochemical tests. 7% of the pathogen Escherichia out of 1049 samples collected were discovered [14].

A research was conducted on the growth of *Shiga Toxin producing Escherichia coli* in uncooked cattle meat. Through Ratkowsky square-root model, it was found that *Shiga Toxin producing Escherichia coli* bacteria increases under minimum temperatures [15].

A study on transmission of Escherichia coli infection through dairy milk was performed. Biochemical tests were used to test fresh cattle dung. Observations showed that Escherichia coli bacterial infections were present in the sample.[16].

A research on how the transmission of *Shiga Toxin producing Escherichia coli* in cattle is influenced by the level of environmental contamination was conducted. The SIS mathematical model was used to estimate and compare the transmission rates. The findings showed that the transmission rate of *Shiga Toxin producing Escherichia coli* increased as the environment contamination rate increased [17].

2. MODEL FORMULATION AND DESCRIPTION

A total population of human beings which vary with time is N(t). It is divided into three categories consisting of people who are susceptible to the diseased S(t), the infected population I(t) and recovered population R(t). The susceptible population move to the infected population either through contact with the infected people at a rate (β) or through contact with the contaminated environment at a rate (ψ). The infected category moves to the recovered population at a rate (α). The recovered population consists of permanent immunity and temporary immunity, the temporary immunity population progresses to the susceptible category at the rate (σ). The natural death rate for all categories is (μ). The death rate due to disease (γ). The recruitment rate of the population in susceptible category is (Λ). The entire population is denoted by N(t) and is given by:

$$N(t) = S(t) + I(t) + R(t) \qquad (1)$$

Figure 1 below represent Shiga Toxin dynamic

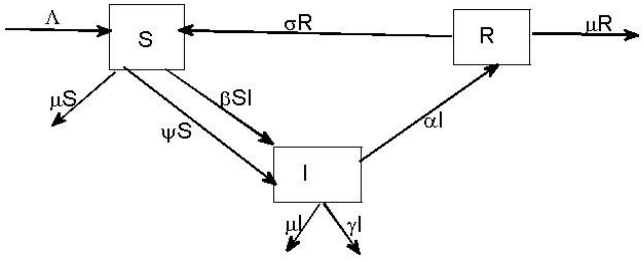

Figure 1: Model Flow

ISSN 2350-1022

International Journal of Recent Research in Mathematics Computer Science and Information Technology
Vol. 7, Issue 1, pp: (32-43), Month: April 2020 – September 2020, Available at: www.paperpublications.org

The differential equations constructed from the model:

$$\frac{dS}{dt} = \Lambda + \sigma R - \beta SI - S(\mu + \psi)$$

$$\frac{dI}{dt} = S(\psi + \beta I) - (\mu + \gamma + \alpha)I$$

$$\frac{dR}{dt} = \alpha I - R(\mu + \sigma)$$

3. DISEASE FREE EQUILIBRIUM

This is the situation in which no disease is present in the populations [8]. At this moment the infectious and recovered sub population will be equal to zero, which means, the susceptible become the total population; so, R(t)=0 and I(t)=0. It is calculated by equating all the differential equations equal to zero.

$$\frac{dS}{dt} = 0$$

$$\frac{dI}{dt} = 0$$

$$\frac{dR}{dt} = 0$$

From the model equations;

$$0 = \Lambda + \sigma R - \beta SI - S(\mu + \psi)$$

$$0 = \beta SI + \psi S - I(\mu + \gamma + \alpha)$$

$$0 = \alpha I - (\sigma + \mu) R$$

At equilibrium; $(S, I, R) = (S^*, I^*, R^*)$ Therefore:

$0 = \Lambda + \sigma R^* - \beta SI^* - S^*(\mu + \psi)$ since $I^* = R^* = 0$ then;

$0 = \Lambda - S^*(\mu + \psi)$

$\Lambda = S^*(\mu + \psi)$

$S^* = \frac{\Lambda}{\psi + \mu}$.

At disease free equilibrium (DFE);

$$(S^*, I^*, R^*) = \left(\frac{\Lambda}{\psi + \mu}, 0, 0\right)$$

Therefore

Disease free equilibrium is $\left(\frac{\Lambda}{\psi+\mu}, 0, 0\right)$

3.1 Stability of the Disease-Free Equilibrium

Theorem 1*: Disease free equilibrium is locally asymptotically stable if $R_0 < 1$ and unstable if $R_0 > 1$ [18]*

Theorem 2*: A necessary and sufficient condition for an equilibrium to be locally asymptotically stable is that, all eigenvalues of the Jacobian have negative real part [6].*

Since disease free equilibrium is $\left(\frac{\Lambda}{\psi+\mu}, 0, 0\right)$

The Stability of DFE is obtained from Jacobian matrix;

$$\begin{pmatrix} -(\beta I^* + \mu + \psi) & -\beta S* & \sigma \\ \beta I^* + \psi & \beta S* - (\mu + \gamma + \alpha) & 0 \\ 0 & \alpha & -(\mu + \sigma) \end{pmatrix}$$

But $S^* = \frac{\Lambda}{\mu+\psi}$, $I^* = 0, R^* = 0$

The characteristic equation given by;

$|J - \lambda I| = 0$

Then J (S*, 0, 0) =

$$\begin{pmatrix} -(\mu + \psi) & -\beta S* & \sigma \\ \psi & \beta S* - (\mu + \gamma + \alpha) & 0 \\ 0 & \alpha & -(\mu + \sigma) \end{pmatrix}$$

The characteristic equations from Jacobians matrix:

$$\mathbf{0} = \begin{vmatrix} -(\mu + \psi) - \lambda & -\beta S* & \sigma \\ \psi & (\beta S* - (\mu + \gamma + \alpha)) - \lambda & 0 \\ 0 & \alpha & -(\mu + \sigma) - \lambda \end{vmatrix}$$

Where λ are eigenvalues

Therefore

$((\mu + \psi) + \lambda)((\mu + \sigma) + \lambda)((\beta S^* - (\mu + \alpha + \gamma)) - \lambda) - \beta S^* \psi((\mu + \sigma) + \lambda) + \sigma\psi\alpha = 0$

$0 = -\lambda^3 + [\beta S^* - (\mu + \alpha + \gamma) - (2\mu + \psi + \sigma)]\lambda^2 + [(\beta S^* - (\mu + \alpha + \gamma))(2\mu + \psi + \sigma) - (\mu + \psi)(\mu + \sigma) - \beta S^* \psi]\lambda$

$+[(\mu + \psi)(\mu + \sigma)((\beta S^* - (\mu + \alpha + \gamma))) - \beta S^* \psi(\mu + \sigma) + \sigma\psi\alpha]\ 0 = \lambda^3 - [\beta S^* - (\mu + \alpha + \gamma) - (2\mu + \psi + \sigma)]\lambda^2 - [(\beta S^* - (\mu + \alpha + \gamma))(2\mu + \psi + \sigma) - (\mu + \psi)(\mu + \sigma) - \beta S^* \psi]\lambda - [(\mu + \psi)(\mu + \sigma)((\beta S^* - (\mu + \alpha + \gamma))) - \beta S^* \psi(\mu + \sigma) + \sigma\psi\alpha]$

$0 = \lambda^3 + [(\mu + \alpha + \gamma) - \beta S^* + (2\mu + \psi + \sigma)]\lambda^2 + [((\mu + \alpha + \gamma) - \beta S^*)(2\mu + \psi + \sigma) + (\mu + \psi)(\mu + \sigma) + \beta S^* \psi]\lambda$

$+[(\mu + \psi)(\mu + \sigma)(\mu + \alpha + \gamma) - (\mu + \psi)(\mu + \sigma)\beta S^* + \beta S^* \psi(\mu + \sigma) - \sigma\psi\alpha]\ 0 = \lambda^3 + [(\mu + \alpha + \gamma)(1 - R_0) + (2\mu + \psi + \sigma)]\lambda^2 + [(\mu + \alpha + \gamma)(1 - R_0)(2\mu + \psi + \sigma) + (\mu + \psi)(\mu + \sigma) + \beta S^* \psi]\lambda + [(\mu + \psi)(\mu + \sigma)(\mu + \alpha + \gamma)(1 - R_0) + \beta S^* \psi(\mu + \sigma) - \sigma\psi\alpha]$

ISSN 2350-1022

International Journal of Recent Research in Mathematics Computer Science and Information Technology
Vol. 7, Issue 1, pp: (32-43), Month: April 2020 – September 2020, Available at: www.paperpublications.org

Theorem 3*: By the principle of Routh Hurwitz criteria, the roots of the polynomial will be negative if and only if the coefficients are positive [19].*

Let the polynomial be, $\lambda^3 + A_1\lambda^2 + A_2\lambda + A_3 = 0$

Where

$A_1 = [(\mu + \alpha + \gamma)(1 - R_0) + 2\mu + \psi + \sigma]$

$A_2 = [(\mu + \alpha + \gamma)(1 - R_0)(2\mu + \psi + \sigma) + (\mu + \psi)(\mu + \sigma) + \beta S^*\psi]$

$A_3 = [(\mu + \alpha + \gamma)(\mu + \psi)(\mu + \sigma)(1 - R_0) + \beta S^*\psi(\mu + \sigma) - \sigma\psi\alpha]$

For the coefficients to be positive, $1 - R_0$ must be positive which leads the $R_0 < 1$.

Therefore, the diseased free equilibrium (DFE) is locally asymptotically stable (L.A.S)

4. BASIC REPRODUCTION NUMBER

It is defined as the average number of secondary cases produced by one infected person introduced into the susceptible population [20].

R_0 is used to measure the spread of disease in the population. If R_0 is less than 1, then the disease-free equilibrium is locally asymptotically stable. The spreading of disease is decreasing. Otherwise is unstable, the rate of spreading is increasing [10]. We compute R_0 by using the concept of next generation matrix [18].

The infectious sub population of the model will be under consideration.

$$\frac{dI}{dt} = S(\psi + \beta I) - (\mu + \gamma + \alpha)I$$

Let $f(x_i)$ be the new infectious in the infected compartment.

Therefore $f(x_i) = \beta SI + \psi S$

$$\frac{\partial f(x_i)}{\partial x_i} = F = \beta S^* \frac{x_i}{\partial x_i} = F = \beta S^*$$

But $S^* = \frac{\Lambda}{\psi+\mu}$ Therefore. $F = \frac{\Lambda}{\psi+\mu}$

Again, we let $Vi^+(x)$ be the rate of shifting of an individual into an infected compartment. $V_i^+(x) = 0$

$V_i^-(x)$ be the rate of an individual transferring out of infected compartment.

$V_i^-(x) = (\mu + \gamma + \alpha)\, I$

So;

$V(x_i) = V_i^-(x) - V_i^+(x)$

Therefore, $V_i(x) = (\mu + \gamma + \alpha)\, I$

$$V = \frac{\partial(V_i(x))}{\partial I} = (\mu + \gamma + \alpha)$$

$$V^{-1} = \frac{1}{(\mu + \gamma + \alpha)}$$

$$R_0 = \rho(FV^{-1})$$

$$R_0 = \frac{\beta\Lambda}{(\psi + \mu)(\mu + \gamma + \alpha)}$$

ISSN 2350-1022

International Journal of Recent Research in Mathematics Computer Science and Information Technology
Vol. 7, Issue 1, pp: (32-43), Month: April 2020 – September 2020, Available at: www.paperpublications.org

5. ENDEMIC EQUILIBRIUM

The endemic equilibrium indicates that, there is spreading of disease in the society. Endemic equilibrium is denoted by E^* where $E^* = (S^*, I^*, R^*)$. To find it, we equate all model differential equations equal to zero. Therefore,

$$\frac{dS}{dt} = 0, \qquad \frac{dI}{dt} = 0, \qquad \frac{dR}{dt} = 0$$

Theorem 4: *A unique endemic equilibrium of a system exists if $R_0 > 1$ [21].*

Proof

$$0 = \Lambda + \sigma R - \beta SI - S(\mu + \psi)$$

$$0 = \beta SI + \psi S - I(\mu + \gamma + \alpha)$$

$$0 = \alpha I - (\sigma + \mu) R$$

$$R^* = \frac{\alpha I^*}{(\sigma + \mu)}$$

substitute R^* in $0 = \Lambda + \sigma R - \beta SI - S(\mu + \psi)$, we get

$$\Lambda + \frac{\sigma \alpha I^*}{\mu + \sigma} - (\beta I^* + \mu + \psi) S^* = 0$$

when we multiply each term by $(\mu + \sigma)$ we obtain

$$S^* = \frac{(\mu+\sigma)\Lambda + \sigma\alpha I^*}{(\mu+\sigma)(\beta I^* + \mu + \psi)}$$

$$\frac{(\psi+\beta I^*)[(\mu+\sigma)\Lambda + \sigma\alpha I^*]}{(\mu+\sigma)(\beta I^* + \mu + \psi)} - (\mu + \gamma + \alpha) I^* = 0$$

Then we multiply through by $(\mu + \sigma)(\beta I^* + \mu + \psi)$ we have

$$0 = (\psi + \beta I^*)[(\mu + \sigma)\Lambda + \sigma\alpha I^*] - (\mu + \sigma)(\beta I^* + \mu + \psi)(\mu + \alpha + \gamma) I^*$$

Then we substitute S^* into; $0 = \beta SI + \psi S - I(\mu + \gamma + \alpha)$

Through expansion and simplification, we obtain

$-[(\mu + \gamma)(\mu + \sigma)\beta + \alpha\mu\beta]$ as the coefficient of I^{*2},

Again

$-[(\mu + \gamma + \alpha)(\mu + \sigma)(\mu + \psi)\{1 - R_0\} - \psi\sigma\alpha]$ as the coefficient of I^* and

$\Lambda\psi(\mu + \sigma)$ as a constant term.

ISSN 2350-1022

International Journal of Recent Research in Mathematics Computer Science and Information Technology
Vol. 7, Issue 1, pp: (32-43), Month: April 2020 – September 2020, Available at: www.paperpublications.org

Therefore, we have

$D2I*2 + D1I* + D0 = 0$

Where

$D_2 = (\mu + \gamma)(\mu + \sigma)\beta + \alpha\mu\beta$

$D_1 = (\mu + \gamma + \alpha)(\mu + \sigma)(\mu + \psi)\{1 - R_0\} - \psi\sigma\alpha$

$D_0 = -\Lambda\psi(\mu + \sigma)$

The endemic equilibrium will exist if the model system has real positive roots. According to Descartes rule of signs [21]. We will observe if there are real positive roots. Since D_2 has positive sign and D_1 has negative sign if $R_0 > 1$, so there is at least one real positive root, then the endemic equilibrium exists.

6. SENSITIVITY ANALYSIS OF PARAMETERS

In this section, the sensitivity analysis of each parameter has been examined. This analysis is performed to show the contribution of each parameter to the basic reproductive number.

Positive values indicate a direct proportional between the given parameter and the R_0. Conversely, when the outcome is negative the implication is an inverse proportional between the parameters and R_0. In order to conclude the effect of changing the size of parameters, the absolute value of the index, in this case can be taken [22].

The sensitivity index of variable Y which depends on a parameter z is defined as: $S_Z^Y = \frac{\partial Y}{\partial Z} * \frac{Z}{Y}$ [3]. where;

Y represents the basic reproductive number and Z represents any parameter in the model. The parameter values used were $\Lambda = 2.5$, $\beta = 0.15$, $\mu = 0.01$, $\alpha = 0.9$, $\sigma = 0.002$, $\gamma = 0.57$, $\psi = 0.28$

The basic reproductive number;

$$R_0 = \frac{\beta\Lambda}{(\psi+\mu)(\mu+\gamma+\alpha)}$$

$$S_\beta^{R_0} = 1$$

$$S_\Lambda^{R_0} = 1$$

$$S_\mu^{R_0} = \frac{-(2\mu+\alpha+\gamma+\psi)\mu}{(\psi+\mu)(\mu+\gamma+\alpha)}$$

$$S_\gamma^{R_0} = \frac{-\gamma}{(\mu+\gamma+\alpha)}$$

$$S_\alpha^{R_0} = \frac{-\alpha}{(\mu+\gamma+\alpha)}$$

$$S_\psi^{R_0} = \frac{-\psi}{(\mu+\psi)}$$

Table 1: Table of sensitivity indices

parameters	Interpretation	indices(+ve/-ve)
Λ	Recruitment rate	+1
μ	Natural mortality rate	-0.04124
γ	death rate due to disease	-0.38514
β	contact rate between susceptible and infected population	+1
ψ	contact rate due to contaminated environment	-0.96552
α	recovered rate	-0.60811

ISSN 2350-1022

International Journal of Recent Research in Mathematics Computer Science and Information Technology
Vol. 7, Issue 1, pp: (32-43), Month: April 2020 – September 2020, Available at: www.paperpublications.org

6.1 Interpretation of the parameter indices

The parameters which have positive indices show the trend of the disease in the society. Their increase depicts an increase in the 'basic reproductive number', and vice versa. It shows that Lambda (Λ) and Beta (β) are the most sensitivity found parameters in R_0. Their increase, therefore implies that R_0 is greater than one ($R_0 > 1$), and their decrease, conversely, indicates the fact that R_0 is less than one ($R_0 < 1$). When the parameters have negative indices therefore impacting on either the decrease or increase of the value of the basic reproductive number.

7. NUMERICAL SIMULATIONS

In this section, numerical simulation of the model equations was used in order to display the impact of contact rate due to contamination on human population. We applied numerical methods and MATLAB ode 45, on which parameter values were used. Table 2 below gives the values of the parameter used.

Table 2: Parameter values

parameters	Interpretation	Values	
Λ	Recruitment rate	2.5	[23]
μ	Natural mortality rate	0.01	[24]
γ	death rate due to disease	0.57	[24]
β	contact rate between susceptible and infected population	0.15	assumed
ψ	contact rate due to contaminated environment	0.28	assumed
α	recovery rate	0.9	[24]
σ	recovered rate progressing to susceptible	0.002	assumed

7.1 Shiga Toxin Infection Dynamics

Figure 7.1 below gives details of the population dynamics with the presence of Shiga toxin amongst the community members. The number of the susceptible decreases as the number of the infectious people increase. The increase in the number of the recovered lags the increase in the infectious population but it surpasses it after the second week leading to flattening of the infectious curve in the fourth week. In the long run, the population is dominated by the recovered population leading to diminishing levels of the infectious population.

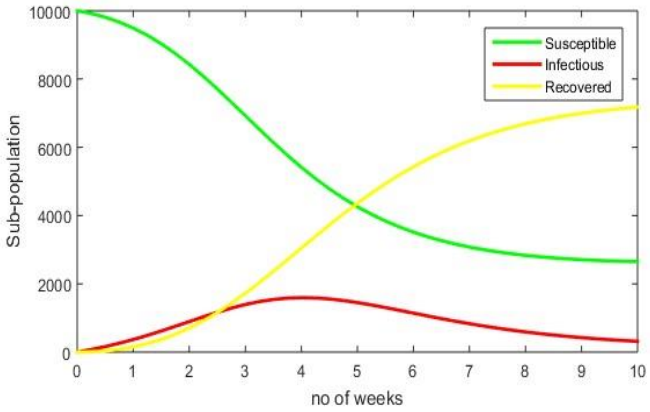

Figure 7.1: Shiga toxin infection dynamics

7.2 Susceptible population dynamics

The population of the susceptible decreases gradually from the initial 10000 due to the increase in the number of infectious people and the recovered individuals as illustrated in figure 7.2 below. The decrease can also be attributed high infection rates and low recruitments rate during the short period of observation. It is clear that most of the people in the community are affected by the infection. This implies that endemic equilibrium is stable as $R_0 > 1$ from figure 3 below. The parameter values used to compute R_0 were

$\Lambda = 2.5$, $\mu = 0.01$, $\gamma = 0.57$, $\beta = 0.25$, $\psi = 0.30$, $\alpha = 0.9$

ISSN 2350-1022

International Journal of Recent Research in Mathematics Computer Science and Information Technology
Vol. 7, Issue 1, pp: (32-43), Month: April 2020 – September 2020, Available at: www.paperpublications.org

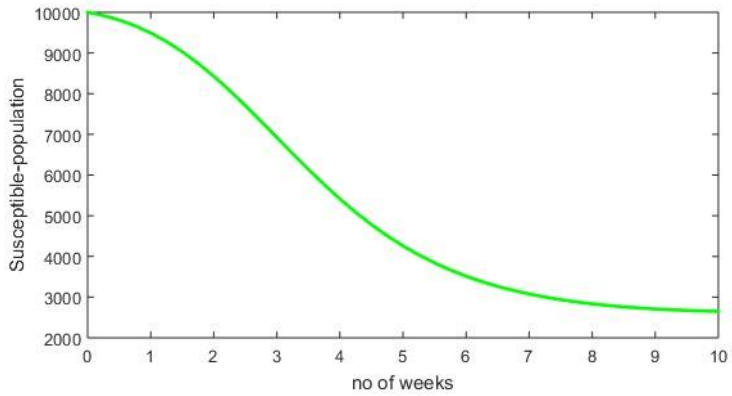

Figure 7.2: R_0 = 1.36225

7.3 Infected population dynamics

The infected population increases rapidly from the incident case to reach a peak of about 1600 people within the first four week. It then decreases gradually over the next six weeks as illustrated in figure 4 below. The population then stabilizes at slightly above 200 people.

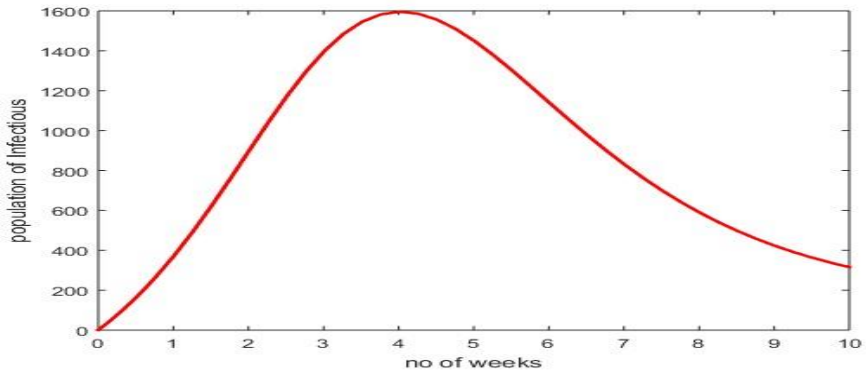

Figure 7.3: Infected population dynamics

7.4 Recovered population dynamics

Figure 7.4 below shows the trend of the recovered population which starts to grow in the first week and grows rapidly between week three and week eight. It then stabilizes in week nine and ten. The graph takes a sigmoid shape. The trend can be attributed to high recovery rates and low mortality rates as a result of the disease. The graph also indicates that most people who get sick recover from the disease. It implies that $R_0 < 1$. The parameter values used to compute R_0 were $\Lambda = 2.5$, $\mu = 0.01$, $\gamma = 0.57$, $\beta = 0.11$, $\psi = 0.20$, $\alpha = 0.9$

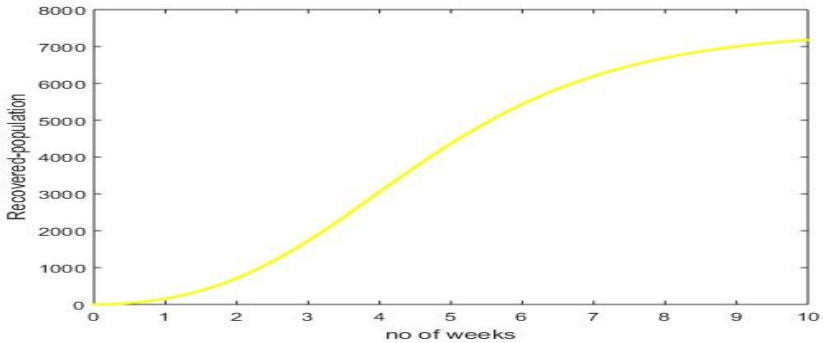

Figure 7.4: R_0 = 0.8848

ISSN 2350-1022

International Journal of Recent Research in Mathematics Computer Science and Information Technology
Vol. 7, Issue 1, pp: (32-43), Month: April 2020 – September 2020, Available at: www.paperpublications.org

7.5 Effect of environment contact rate on the infectious population

The rate of infection decreases significantly at the environmental contact rate, represented in the model by ψ, decreases. A decrease the environmental contact rate decreases the peak of the infectious population. It also lags the peak of the infectious population giving more time for effective interventions to be enacted to better manage the disease as illustrated in figure 7.5 below

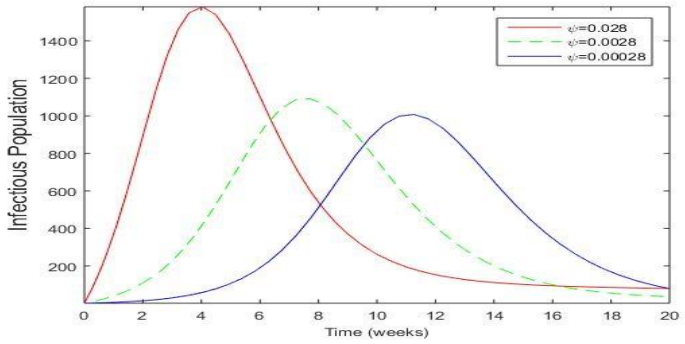

Figure 7.5: Infectious population Under different values of ψ

7.6 Effect of environment contact rate on the susceptible population

Figure 7.6 shows that a decrease in the environmental contact rate leads to an increase in the susceptible population. This is attributed to low infection rates during low environmental contact rates thus leading to less people getting infected.

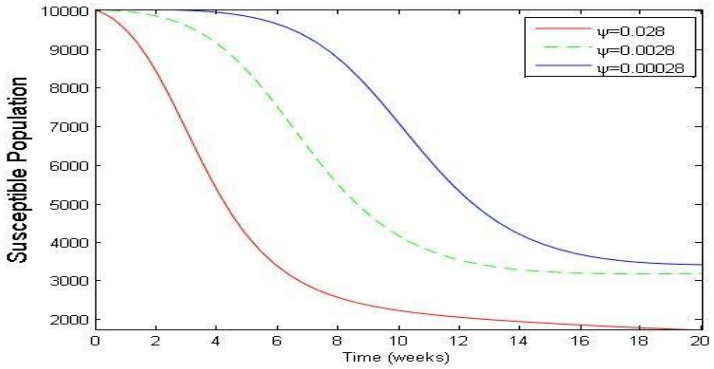

Figure 7.6: Susceptible population under different values of ψ

7.7 Effect of environment contact rate on the recovered population

As the environment contact rate decreases the recovered population decreases since less people get infected. This trend is illustrated in the figure 7.7 below.

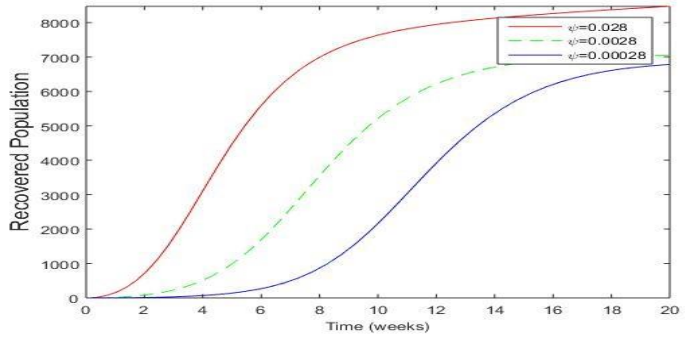

Figure 7.7: Recovered population under different values of ψ

8. CONCLUSION

In this project, we composed and analysed mathematical modelling of Shiga toxin incorporating the environment. The Basic Reproductive number (R_O) was obtained by use of the Next Generation Approach, and through it the model stabilities were determined. The sensitivity analysis of each parameter has been obtained. It shows that Lambda (Λ) and Beta (β) are the most sensitivity found parameters in R_0. Their increase, therefore implies that R_0 is greater than one ($R_0 > 1$), and their decrease, conversely, indicates the fact that R_0 is less than one ($R_0 < 1$).

The rest of the parameters have negative indices, therefore impacting on either the decrease or increase of the value of the basic reproductive number.

Numerical simulation was used to show the different behaviour of the compartments. The trajectories from the model illustrate that as the environmental contact rate (Ψ) increases, the susceptible trajectory decreases and consequently the infectious trajectory increases. Conversely, when the environmental contact rate decreases the susceptible trajectory increases. Epidemiologically, epidemic persists when $R_0 > 1$ and the disease will be eliminated if $R_0 < 1$.

9. DATA AVAILABILITY

The data used in the analysis of the model were obtained from previously published articles and which have been cited accordingly. Some of the parameter values are assumed and others are taken from published articles. These articles are cited at relevant places within the text as references.

CONFLICT OF INTEREST

The authors of this publication declare that there is no conflict of interest regarding the publication of this manuscript.

REFERENCES

[1] Valcour, J. E., Michel, P., McEwen, S. A., & Wilson, J. B. (2002). Associations between indicators of livestock farming intensity and incidence of human Shiga toxin-producing Escherichia coli infection. Emerging infectious diseases, 8(3), 252.

[2] Chase-Topping, M. Gally, D. Low, C. Matthews, L. & Woolhouse, M. (2008). Super-shedding and the link between human infection and livestock carriage of Escherichia coli O157. Nature Reviews Microbiology, 6(12), 904-912

[3] Osman, S., Makinde, O. D., & Theuri, D. M. (2018). Stability analysis and modelling of listeriosis dynamics in human and animal populations. Global journal of pure and Applied Mathematics, 14(1), 115-137.

[4] Scallan, E., Hoekstra, R. M., Angulo, F. J., Tauxe, R. V., Widdowson, M. A., Roy, S. L., & Griffin, P. M. (2011). Foodborne illness acquired in the United States-major pathogens. Emerging infectious diseases, 17(1), 7.

[5] Robinson, A. P. L., Gibbon, P., Zepf, M., Kar, S., Evans, R. G., & Bellei, C. (2009). Relativistically correct hole-boring and ion acceleration by circularly polarized laser pulses. Plasma Physics and Controlled Fusion, 51(2), 024004.

[6] Nyasagare, B. N., Osman, S., & Wainaina, M. (2019). Modelling and Analysis of Campylobacteriosis in Human and Animal Populations. Global Journal of Pure and Applied Mathematics, 15(5), 551-567.

[7] Mukherjee, A., Speh, D., & Diez-Gonzalez, F. (2007). Association of farm management practices with risk of Escherichia coli contamination in pre-harvest produce grown in Minnesota and Wisconsin. International journal of food microbiology, 120(3), 296-302.

[8] Muia, D.W., Osman, S. & Wainaina, M. (2018) Modelling and analysis of trypanosomiasis transmission mechanism Global Journal of Pure and Applied Mathematics, 14(10), 1311-1331.

[9] Majowicz, S. E., Musto, J., Scallan, E., Angulo, F. J., Kirk, M., O'Brien, S. J. & International Collaboration on Enteric Disease "Burden of Illness" Studies. (2010). The global burden of nontyphoidal Salmonella gastroenteritis. Clinical infectious diseases, 50(6), 882-889.

[10] Eustace, K. A., Osman, S., & Wainaina, M. (2018). Mathematical modelling and analysis of the dynamics of cholera. Global Journal of Pure and Applied Mathematics, 14(9), 1259-1275.

[11] Jones, N. L., Islur, A., Haq, R., Mascarenhas, M., Karmali, M. A., Perdue, M. H. & Sherman, P. M. (2000). Escherichia coli Shiga toxins induce apoptosis in epithelial cells that is regulated by the Bcl-2 family. American Journal of Physiology-Gastrointestinal and Liver Physiology, 278(5), G811-G819

[12] Schlager, S. Lepuschitz, S. Ruppitsch, W. Ableitner, O. Pietzka, A., Neubauer, S. & Allerberger, F. (2018) Petting zoos as sources of Shiga toxin-producing Escherichia coli (STEC) infections. International Journal of Medical Microbiology, 308(7), 927-932.

[13] Muniesa, M., Hammerl, J. A., Hertwig, S., Appel, B. & BrÃOEssow, H. (2012). Shiga toxin-producing Escherichia coli O104: H4: a new challenge for microbiology. Appl. Environ. Microbiol., 78(12), 4065-4073.

[14] Lupindu, A. M. Olsen, J. E. Ngowi, H. A., Msoffe, P. L., Mtambo, M. M., Scheutz, F. & Dalsgaard, A. (2014).Occurrence and characterization of shiga toxin-Producing Escherichia coli O157: H7 and other non-sorbitol-fermenting E. coli in cattle and humans in urban areas of Morogoro, Tanzania. Vector-Borne and Zoonotic Diseases, 14(7), 503-510.

[15] Huang, L., Tu, S. I., Phillips, J. & Fratamico, P. (2012). Mathematical Modeling of Growth of Non-O157 Shiga Toxin-Producing Escherichia coli in Raw Ground Beef. Journal of food science, 77(4), M217-M225.

[16] Rachmawati, F., & Ariyanti, T. (2018). Contamination of Escherichia coli O157: H7 in dairy cow farms. Journal Ilmu Ternak dan Veteriner, 22(4), 205-211.

[17] Gautam, R., Kulow, M., Park, D., Gonzales, T. K., Dahm, J., Shiroda, M., & Ivanek, R. (2015). Transmission of Escherichia coli O157: H7 in cattle is influenced by the level of environmental contamination. Epidemiology & Infection, 143(2), 274-287.

[18] Van den Driessche, P., & Watmough, J. (2002). Reproduction numbers and subthreshold endemic equilibria for compartmental models of disease transmission. Mathematical biosciences, 180(1-2), 29-48.

[19] DeJesus, E. X., & Kaufman, C. (1987). Routh-Hurwitz criterion in the examination of eigenvalues of a system of nonlinear ordinary differential equations. Physical Review A, 35(12), 5288.

[20] Heffernan, J. M., Smith, R. J., & Wahl, L. M. (2005). Perspectives on the basic reproductive ratio. Journal of the Royal Society Interface, 2(4), 281-293.

[21] Wang, X. (2004). A simple proof of Descartes's rule of signs. The American Mathematical Monthly, 111(6), 525.

[22] Edward, S., & Nyerere, N. (2016). Modelling typhoid fever with education, vaccination and treatment. Eng. Math, 1(1), 44-52.

[23] Obuya J. O, Kimathi G. & Kaluki W. (2020). Incorporporating Sensitization in Mathematical Modelling of Alcoholism as an Infectious Disease. International Journal of Novel Research in Physics, Chemistry and Mathematics. Vol.7, Issue 2, pp (8-18), Month: May – August 2020.

[24] Wangari I. M. and Stone L. (2017). Analysis of a heroin epidemic model with saturated treatment function. Journal of Applied Mathematics, 2017.